

## Hijacking of the Human Alkyl-*N*-purine-DNA Glycosylase by 3,*N*<sup>4</sup>-Ethenocytosine, a Lipid Peroxidation-induced DNA Adduct\*<sup>§</sup>

Received for publication, December 22, 2003, and in revised form, January 29, 2004  
Published, JBC Papers in Press, February 2, 2004, DOI 10.1074/jbc.M314010200

Laurent Gros<sup>‡</sup>, Andrei V. Maksimenko, Cyril V. Privezentzev<sup>‡,§</sup>, Jacques Laval,  
and Murat K. Sagarbaev<sup>¶</sup>

From the Groupe "Réparation de l'ADN," CNRS Unité Mixte de Recherche 8113/LBPA-ENS Cachan, Institut Gustave Roussy, 39, rue Camille Desmoulins, 94805 Villejuif Cedex, France

Lipid peroxidation generates aldehydes, which react with DNA bases, forming genotoxic exocyclic etheno( $\epsilon$ )-adducts. E-bases have been implicated in vinyl chloride-induced carcinogenesis, and increased levels of these DNA lesions formed by endogenous processes are found in human degenerative disorders. E-adducts are repaired by the base excision repair pathway. Here, we report the efficient biological hijacking of the human alkyl-*N*-purine-DNA glycosylase (ANPG) by 3,*N*<sup>4</sup>-ethenocytosine ( $\epsilon$ C) when present in DNA. Unlike the etheno-purines, ANPG does not excise, but binds to  $\epsilon$ C when present in either double-stranded or single-stranded DNA. We developed a direct assay, based on the fluorescence quenching mechanism of molecular beacons, to measure a DNA glycosylase activity. Molecular beacons containing modified residues have been used to demonstrate that the  $\epsilon$ C-ANPG interaction inhibits excision repair both in reconstituted systems and in cultured human cells. Furthermore, we show that the  $\epsilon$ C-ANPG complex blocks primer extension by the Klenow fragment of DNA polymerase I. These results suggest that  $\epsilon$ C could be more genotoxic than 1,*N*<sup>6</sup>-ethenoadenine ( $\epsilon$ A) residues *in vivo*. The proposed model of ANPG-mediated genotoxicity of  $\epsilon$ C provides a new insight in the molecular basis of lipid peroxidation-induced cell death and genome instability in cancer.

tion, which target DNA bases forming genotoxic exocyclic adducts such as 1,*N*<sup>6</sup>-ethenoadenine ( $\epsilon$ A) and 3,*N*<sup>4</sup>-ethenocytosine ( $\epsilon$ C) (1–3). Etheno( $\epsilon$ )-adducts are also formed by reaction with epoxides that result from the metabolism of various industrial pollutants such as vinyl chloride and vinyl carbamate (4). E-adducts are ubiquitous, and highly variable background levels of  $\epsilon$ A and  $\epsilon$ C were found in asymptomatic tissue DNA under normal physiological conditions. It was shown that the level of  $\epsilon$ C present in 10 different human liver DNA samples averaged  $28 \pm 9 \epsilon$ C/ $10^8$  bases (5), whereas in leukocytes, pancreas, and colon DNA samples isolated from healthy volunteers, it ranged from 0.1 to  $11 \epsilon$ C/ $10^8$  parent bases (6). Based on these numbers, we estimate that the molar concentration of  $\epsilon$ C within the nucleus in human cells ranges from 0.2 to 40 nM. The low density lipids that transport cholesterol in the bloodstream are extremely susceptible to oxidation (7), and it was speculated that this may account for the highly variable background levels of  $\epsilon$ -adducts found in the DNA from normal human tissues (1).

The increasing interest in exocyclic DNA adducts has been triggered by the observation that they are highly mutagenic. During DNA replication in *Escherichia coli* and simian kidney cells,  $\epsilon$ C mostly produces  $\epsilon$ C·G to A·T transversions and  $\epsilon$ C·G to T·A transitions (8, 9). In a single-stranded shuttle vector containing a single  $\epsilon$ C residue, the targeted mutation frequency yield was 81% in simian kidney cells (9). The  $\epsilon$ A residues are also highly mutagenic in mammalian cells, where they lead mainly to  $\epsilon$ A·T to T·A transversions (10, 11) but are weak mutagens in *E. coli*. Therefore, the processes preventing mutations caused by  $\epsilon$ -adducts in the genome upon cell division should play a crucial role in maintaining the stability of the genetic information. When present in DNA,  $\epsilon$ C residues are eliminated by the base excision repair (BER) pathway initiated in human cells by mismatch-specific thymine-DNA glycosylase (hTDG) (12, 13). However, excision efficiency of  $\epsilon$ C by hTDG is rather poor (12). Recently, two additional enzymes that excise  $\epsilon$ C, have been identified in human cells: the methyl-CpG binding domain protein (MBD4/MED1) (14) and single-strand monofunctional uracil-DNA glycosylase (SMUG1) (15).

Oxidative stress generates reactive aldehydes, as a by-product of lipid peroxidation (LPO)<sup>1</sup> and nitric oxide overproduc-

\* This work was supported by grants (to M. K. S. and J. L.) from the European Community QLK4-2000-00286 and RISC-RAD FI6R-CT-2003-508842, Association pour la Recherche sur le Cancer, a grant from the Electricité de France Contrat Radioprotection (to M. K. S.), and a grant from the Fondation Franco-Norvégienne pour la Recherche Scientifique et Technique et le Développement Industriel (J. L.). The costs of publication of this article were defrayed in part by the payment of page charges. This article must therefore be hereby marked "advertisement" in accordance with 18 U.S.C. Section 1734 solely to indicate this fact.

<sup>§</sup> The on-line version of this article (available at <http://www.jbc.org>) contains supplementary figures showing inhibition of a DNA glycosylase activity by 3,*N*<sup>4</sup>-ethenocytosine in the reconstituted system and in the cultured mouse cells.

<sup>‡</sup> Supported by a postdoctoral fellowship from the European Community.

<sup>§</sup> Present address: Dept. of Biochemistry and Molecular Biology, University College London, London, WC1E 6BT UK.

<sup>¶</sup> To whom correspondence should be addressed: Tel.: 33-1-42-11-54-04; Fax: 33-1-42-11-52-76; E-mail: [smurat@igr.fr](mailto:smurat@igr.fr).

<sup>1</sup> The abbreviations used are: LPO, lipid peroxidation;  $\epsilon$ , etheno;  $\epsilon$ A, 1,*N*<sup>6</sup>-ethenoadenine;  $\epsilon$ C, 3,*N*<sup>4</sup>-ethenocytosine; 1,*N*<sup>2</sup>- $\epsilon$ G, 1,*N*<sup>2</sup>-ethenoguanine; Hx, hypoxanthine; I, inosine; THF, tetrahydrofuran; 8-oxoG, 7,8-dihydro-8-oxoguanine; DHU, 5,6-dihydrouracil; DHT, 5,6-dihydrothymine; 5ohU, 5-hydroxyuracil; AP, apurinic/apyrimidinic; BER, base

excision repair; TagI, *E. coli* 3-methyladenine-DNA-glycosylase I; AlkA, *E. coli* 3-methyladenine-DNA-glycosylase II; UDG, *E. coli* uracil-DNA-glycosylase; Fpg, *E. coli* formamidopyrimidine-DNA glycosylase; Nth, *E. coli* endonuclease III; Nfo, *E. coli* endonuclease IV; MUG, mismatch-specific uracil-DNA glycosylase; ANPG, human alkylpurine-DNA N-glycosylase; APDG, rat ANPG; hOGG1, human 7,8-dihydro-8-oxoguanine-DNA glycosylase; hNth1, human endonuclease III; Ape1, human AP-endonuclease; hTDG, human thymine-DNA glycosylase; BSA, bovine serum albumin; FITC, fluorescein isothiocyanate; EMSA, electrophoretic mobility shift assay; SPR, surface plasmon resonance; dabcy1, 4-(4-dimethylaminophenyl-azo)benzoic acid; XPA and XPC, *Xeroderma pigmentosum* complementation group A and C.

The human alkyl-*N*-purine-DNA glycosylase (ANPG) excises  $\epsilon$ A and a variety of damaged bases including alkylated purines, hypoxanthine (Hx) and 1,*N*<sup>2</sup>-ethenoguanine (1,*N*<sup>2</sup>- $\epsilon$ G), but it does not excise  $\epsilon$ C (reviewed in Ref. 16). Rat and murine homologs of ANPG have also been characterized (17, 18). Studies using ANPG-deficient mice (*Aag*) suggest that ANPG could be an important determinant of cellular sensitivity to alkylating agents. *Aag*<sup>-/-</sup> mouse embryonic stem cells and fibroblasts show an increased sensitivity to methyl methanesulfonate and antitumor agents such as mitomycin C and *N*-methylnitrosourea (19, 20). Moreover, *Aag*<sup>-/-</sup> splenic T lymphocytes show a significant increase in methyl methanesulfonate-induced mutations when compared with the wild type (21). However, surprisingly, *Aag*<sup>-/-</sup> myeloid progenitor bone marrow cells show an unexpected resistance to alkylation damage (22), and pancreatic  $\beta$  cells of *Aag* null mice exhibit a markedly decreased susceptibility to necrosis induced by streptozotocin (23). Thus, in particular cell types, sensitivity to alkylating agents could be related to ANPG status.

The ANPG protein in normal human breast cells is localized in the nucleus as shown by immunofluorescent staining (24). In human cells, ANPG could be present as several alternatively spliced forms, including a truncated version (25–27); consequently, it has been concluded that the non-conserved, N-terminal region apparently contributes little to the damage recognition and *N*-glycosylase activity (28). However, we have recently demonstrated that the first N-terminal 80 amino acids of ANPG are essential for 1,*N*<sup>2</sup>- $\epsilon$ G-DNA glycosylase activity (29). Previous reports have indicated that ANPG can recognize some modified bases without excising them. Based on gel retardation assays, ANPG was found to interact with a pyrrolidine abasic site analog (30), and a phenotypic complementation study suggested that it could interact with 7,8-dihydro-8-oxoguanine (8-oxoG) (31), although the pure protein does not excise 8-oxoG. Moreover, it has been shown that ANPG recognizes cisplatin-DNA adducts in a reconstituted system with mild affinity ( $K_D$  71–144 nM) and may shield these adducts from repair by blocking the access to other proteins (32).

Current methods to measure the DNA glycosylase activities are indirect and time-consuming. To overcome these limits, we developed a method based on molecular beacons containing modified bases that allows direct and high throughput DNA glycosylase assay in reconstituted systems and in cultured cells. The molecular beacon is a single-stranded oligonucleotide probe containing a sequence complementary to the target that is flanked by self-complementary termini, and it carries a fluorophore and a quencher at the 5'- and 3'-ends (33). In the absence of the DNA target, these molecules form a stem-loop structure in which the 5'-fluorophore and 3'-quencher are in close proximity to each other, causing the fluorescence of the fluorophore to be quenched by fluorescence resonance energy transfer (34). Here, we report that excision of modified bases present in molecular beacon by a DNA glycosylase can be detected by increase in fluorescence.

In the present work, a search for specific inhibitors of ANPG revealed that the human and rat proteins bind specifically to  $\epsilon$ C residues present in either duplex or single-stranded oligonucleotides. This abortive interaction between ANPG and  $\epsilon$ C residues strongly inhibits Hx and  $\epsilon$ A-DNA glycosylase activity in the reconstituted systems. Furthermore, using a modified molecular beacon, we demonstrated that short oligonucleotide duplex containing a single  $\epsilon$ C residue inhibits ANPG activity in cultured human and mouse cells. In addition, the  $\epsilon$ C-ANPG complex strongly inhibits both  $\epsilon$ C excision by hTDG and DNA synthesis by Klenow fragment in primer extension assays.

Taken together, these results suggest that hijacking of ANPG in the  $\epsilon$ C-ANPG complex may lead to the persistence of  $\epsilon$ C *in vivo* and could result in replication fork arrest. The importance of the present observation is underlined by the fact that hijacking of cellular proteins by DNA damage has been implicated in the action of cisplatin drugs (35) and the expansion of trinucleotide repeats in Huntington disease (36). Here, we propose a model of enhanced genotoxicity of the  $\epsilon$ C adduct. The possible implications of the  $\epsilon$ C-ANPG interaction for LPO-induced cytotoxicity and genome instability are discussed.

#### EXPERIMENTAL PROCEDURES

**Oligonucleotides**—All oligodeoxyribonucleotides were purchased from Eurogentec (Seraing, Belgium) and Genset (Evry, France) including the following oligonucleotides: modified,  $\epsilon$ A, d(AATTGCTATCTAGCTCCGC- $\epsilon$ A-CGCTGGTACCCATCTCATGA)-biotin;  $\epsilon$ A2, d(AATTACATCGTCACTGGG- $\epsilon$ A-CATGTTGCAGATCCATGCAC);  $\epsilon$ C40, d(AATTGCTATCTAGCTCCGC- $\epsilon$ C/C-CGCTGGTACCCATCTCATGA)-biotin; M13- $\epsilon$ C or M13-C, d(CTATTAACGCCAGCTGG- $\epsilon$ C/C-AAATGGGGGATGTGCTGCAAGGCG);  $\epsilon$ C- or C-hairpin d(TGGG- $\epsilon$ C/C-CATGCTGGCCCA); X, d(AAATACATCGTCACTGGG-X-CATGTTGCAGATCC), where X is cytosine (C), mismatched thymine (T), uracil (U),  $\epsilon$ A,  $\epsilon$ C, tetrahydrofuran, an abasic site analog (THF), 8-oxoG, 5,6-dihydrouracil (DHU), 5,6-dihydrothymine (DHT), inosine (I), or 5-hydroxyuracil (5ohU); molecular beacons, 35F-control, FITC-d(GCACCTAAGAATTC-ACGCCATGTGCGAAATCTTAAGTGC); 35FD-control, FITC-d(GCACCTAAGAATTCACGCCATGTGCGAAATCTTAAGTGC)-dabcyl, where FITC is fluorescein isothiocyanate and dabcyl is 4-(4'-dimethylaminophenylazo)benzoic acid; non-modified, PR-13, d(CGCCTTGCAGCAC); FLAP 7.6, d(TAGAGGCCATTTGCCAGCTGGCGTAATAG); complementary oligonucleotides, containing dA, dG, dC, or T opposite to modified base. Molecular beacon oligonucleotide, inosine-FD, FITC-d(CGCITCIACICIT-(CH<sub>2</sub>)<sub>18</sub>-ACICITCIACICG)-dabcyl, was a gift from Dr Y. Alekseev. To obtain duplex DNA, a modified oligonucleotide was hybridized to its complement, and the resulting oligonucleotide duplexes are referred to as X·C(G,A,T), respectively, where X is a modified base. The sequence contexts were used previously to study the repair of  $\epsilon$ -adducts and hypoxanthine (29, 37). Oligonucleotides were 5'-end labeled by T4 polynucleotide kinase (New England Biolabs, OZyme, Saint Quentin Yvelines, France) in the presence of [ $\gamma$ -<sup>32</sup>P]ATP (4500 Ci/mmol, ICN Biomedicals, S.A.R.L., Orsay, France).

**Cell Lines and Culture**—Lich cells are derived from a human hepatoma (38). Lich, HeLa, and NIH3T3 cells were respectively grown in minimum essential medium and in Dulbecco's modified Eagle's medium (Invitrogen) at 37 °C in a humidified atmosphere with 5% CO<sub>2</sub>. Culture media were supplemented with 10% heat-inactivated fetal calf serum (Invitrogen), 100  $\mu$ g/ml streptomycin, and 100 units/ml penicillin. Cell-free extracts were prepared as described (38).

**Enzymes**—Purification of the *E. coli* UDG (uracil-DNA glycosylase), TagI (3-methyladenine-DNA glycosylase I), AlkA (3-methyladenine-DNA glycosylase II), MUG (mismatch-specific uracil-DNA glycosylase), Fpg (formamidopyrimidine-DNA glycosylase), Nth (endonuclease III), Nfo (endonuclease IV), hTDG (human mismatch-specific thymine-DNA glycosylase), hOGG1 (human 8-oxoG-DNA glycosylase), ANPG70, ANPG60, ANPG40, and ANPG80 proteins was performed as described (29). Purification of *Saccharomyces cerevisiae* Apn1 (apurinic/apyrimidinic (AP) endonuclease 1) and human AP endonuclease 1 (Ape1) proteins was performed as described (39). Human Nth1 (human endonuclease III) protein was generously provided by Dr. R. Roy (American Health Foundation, Valhalla, NY). The activity of the various proteins was tested using their principal substrates and was checked just prior to use.

**Enzyme Assays**—The release of  $\epsilon$ A,  $\epsilon$ C, and thymine residues was measured by the cleavage of an oligonucleotide containing a single lesion at a defined position. The standard assay for  $\epsilon$ C and thymine excision activity (20  $\mu$ l) contained 0.2 pmol of the 5'-<sup>32</sup>P-end labeled oligonucleotide duplex, 70 mM Hepes-KOH, pH 7.8, 1 mM EDTA, 5 mM 2-mercaptoethanol, 100  $\mu$ g/ml BSA, and limiting amounts of enzyme, unless otherwise stated. The reaction mix for  $\epsilon$ A excision activity was supplemented with 100 mM KCl. Incubations were carried out at 37 °C except for hTDG, which was at 30 °C. The abasic sites were revealed by light piperidine treatment (10% piperidine at 37 °C for 15 min) (40), and reaction products were analyzed as described (39). The gels were exposed to a Storm 840 Phosphor Screen, and the amounts of radioactivity in the bands were quantified using ImageQuant™ software. The standard enzyme assay with molecular beacon was performed at 37 °C

with 5–35 nM oligonucleotides and a limited amount of protein, in the respective reaction buffer. Reactions were performed in a quartz cuvette (final volume, 0.4 ml), and fluorescence was measured using an SFM 25 Kontron fluorimeter and real-time computed with the attached software WIND25 1.50. Excitation was at 488 nm, and emission was at 515 nm. Fluorescence was expressed as response units. At the end of the reaction, to compare the fluorescence of the reaction product with that of the reaction mixture without enzyme, emission spectra of the reaction product and the reaction mixture without enzyme were obtained between 500 and 550 nm and with an excitation at 488 nm.

**Electrophoretic Mobility Shift Assay (EMSA)**—The standard binding reaction mixture (20  $\mu$ l) contained 70 mM Hepes-KOH, pH 7.8, 1 mM EDTA, 100 mM KCl, 5 mM 2-mercaptoethanol, 20–200 fmol of 5'-<sup>32</sup>P-labeled oligonucleotide duplex, limiting amounts of protein, and non-labeled competitor oligonucleotide, unless otherwise stated. The mixture was incubated for 20 min on ice, after which an aliquot was analyzed by electrophoresis on a 10% non-denaturing polyacrylamide gel (37.5:1 acrylamide/bisacrylamide) using 0.5 $\times$  Tris-borate-EDTA buffer (45 mM Tris borate, pH 8, 1 mM EDTA) at 4 mA/100 V for 14 h at +4  $^{\circ}$ C. The gels were analyzed as described above.

**Surface Plasmon Resonance Techniques**—Kinetics of interaction were determined using a BIAcore 1000 instrument (Biacore AB, Uppsala, Sweden). Pre-annealed, biotinylated oligonucleotide duplex  $\epsilon$ C40-G (0.1 ng/ $\mu$ l in Hepes buffered saline-EDTA polysorbate buffer containing: 10 mM Hepes-KOH, pH 7.4, 500 mM NaCl, 3.4 mM EDTA, 0.005% (v/v) polysorbate 20) was injected at flow rate of 2  $\mu$ l/min onto a streptavidin-coated sensor chip (SA sensor chip, Biacore). To remove non-specifically bound material, 30  $\mu$ l of 0.05% SDS was pulsed. The amount of immobilized ligand was found to be about 600–900 response units. To determine dissociation equilibrium constants ( $K_D$ ) using surface plasmon resonance (SPR), the 40-mer duplex containing  $\epsilon$ C was immobilized onto the sensor chip surface as described, and then different concentrations of ANPG40 were injected in low salt Hepes buffered saline-EDTA polysorbate buffer containing only 150 mM NaCl at a flow rate 30  $\mu$ l/min. At the end of the association time, dissociation was achieved by injecting the same buffer. Analysis of the sensorgrams and  $K_D$  values were performed using BIAevaluation software.

**DNA Repair Assay in Cultured Cells**—HeLa and NIH3T3 cells were grown in 6-well plates. Cells were washed two times with phosphate-buffered saline, and culture medium was replaced by 1 ml of OptiMEM medium (Invitrogen) before transfection. 200 pmols of each oligonucleotide and 2  $\mu$ g of Cytofectin GSV (Glen Research, Sterling, VA) were diluted separately in 50  $\mu$ l of solution A (100 mM NaCl, 10 mM Hepes, pH 7.4) and then mixed together. After 15 min of incubation at room temperature, cytofectin:DNA complexes were added drop by drop to the cells, which were grown for 5 h and then fixed with a 4% formaldehyde solution for 20 min at 4  $^{\circ}$ C before examination in a fluorescence microscope.

**Primer Extension Assay**—To generate a double-stranded matrix for DNA synthesis, a 41-mer oligonucleotide template containing either  $\epsilon$ C (M13- $\epsilon$ C) or C (M13-CC) at position 17 was annealed to a 5'-<sup>32</sup>P-labeled 13-mer primer (PR13) and a partially complementary 29-mer (Flap 7.6) oligonucleotide at a 1:1.2 molar ratio by heating to 95  $^{\circ}$ C for 5 min and slow cooling. The standard reaction mixture (20  $\mu$ l) contained 10 mM 5'-<sup>32</sup>P primer/template, 10 mM Tris-HCl, pH 7.5, 1 mM dithiothreitol, 5 mM MgCl<sub>2</sub>, 100  $\mu$ M each of dNTP and 1 unit of Klenow fragment. Where stated, 20–500 nM ANPG80 and/or ANPG70 were added. Reactions were performed at 37  $^{\circ}$ C for 5 min, and products were analyzed as described above.

## RESULTS

**Effect of Duplex Oligonucleotides Containing Single Modified Base upon  $\epsilon$ A-DNA Glycosylase Activity of ANPG**—In a search for specific inhibitors of ANPG, we measured the  $\epsilon$ A-DNA glycosylase activity of ANPG in the presence of a competitor duplex oligonucleotide containing specific base modifications. The 5'-<sup>32</sup>P-labeled  $\epsilon$ A-T was incubated with purified ANPG70 protein in the absence or presence of a molar excess of the following non-labeled duplex oligonucleotides: C-G, G-T, G-U,  $\epsilon$ A-T,  $\epsilon$ C-G, THF-G, 8-oxoG-C (Fig. 1A) and 8-oxoG-A, DHU-G, DHT-A, I-T 5ohU-G (data not shown) at 37  $^{\circ}$ C for 20 min. As shown in Fig. 1A, when  $\epsilon$ A-T is treated with ANPG70 followed by light piperidine, in order to reveal abasic sites generated by ANPG, about 70% of the oligonucleotide was incised (lane 2). Equimolar amount of non-labeled (cold)  $\epsilon$ A-T and I-T oligonu-

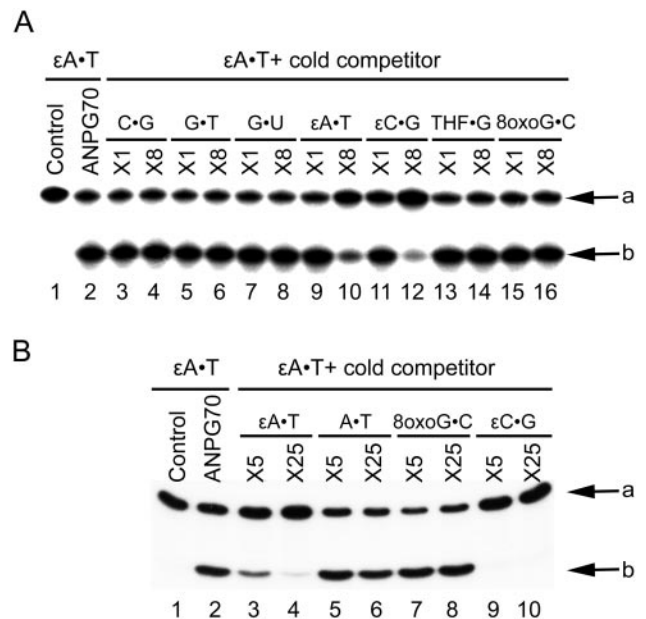


**FIG. 1. Effect of various modified oligonucleotide duplexes on  $\epsilon$ A-DNA glycosylase activity of the purified ANPG protein and in Lich cells extract.** A, purified ANPG70 protein. Prior to the reaction, ANPG70 was incubated with respective competitor DNA (10–80 nM) for 30 min at 0  $^{\circ}$ C. The reaction mixtures, with 10 nM 5'-<sup>32</sup>P-labeled  $\epsilon$ A-T, were incubated for 20 min at 37  $^{\circ}$ C. B, Lich cells extract. 4 nM 5'-<sup>32</sup>P-labeled  $\epsilon$ A2-T was incubated with Lich cell extract (100  $\mu$ g) for 60 min at 37  $^{\circ}$ C in the absence (lane 2) or in the presence of a non-labeled competitor DNA (lanes 3–10). Reaction products were analyzed as described under "Experimental Procedures." a and b indicate 40- and 19-mer fragments.

cleotides had a very slight, if any, inhibition effect (lane 9 and data not shown). However, an 8-fold molar excess of  $\epsilon$ A-T lead to a 4-fold reduction of  $\epsilon$ A excision (lane 10). The weak inhibition by  $\epsilon$ A-T and I-T might be due to the high  $K_m$  value of ANPG for these substrates (24 and 69 nM, respectively) (41, 42). No significant effect on  $\epsilon$ A-DNA glycosylase activity of ANPG was detected in the presence of C-G, G-T, G-U, THF-G, 8-oxoG-C, 8-oxoG-A, 5ohU-G, DHU-G, DHT-A, and I-T oligonucleotides, even at 8-fold molar excess (lanes 3–8, lanes 13–16, and data not shown). 2- and 20-fold reductions of the incision were observed in the presence of 1- and 8-fold molar excess of  $\epsilon$ C-G, respectively (lanes 11–12), indicating that  $\epsilon$ C is a more efficient inhibitor than  $\epsilon$ A (or Hx) (lanes 10 and 12). Similar results were obtained when the truncated ANPG40 and rat APDG60 were used, indicating that the non-conserved N-terminal region does not contribute to the substrate specificity (not shown) and that both the human and the rat ANPG proteins can form a specific interaction with  $\epsilon$ C. Identical patterns of inhibition were obtained with  $\epsilon$ A2-T oligonucleotide duplex, which has different sequence context than  $\epsilon$ A-T, indicating that the  $\epsilon$ C-G effect is not sequence-specific. Furthermore, the Hx- and 3-methyladenine-DNA glycosylase activities of ANPG were also strongly inhibited in the presence of a 3- and 6-fold molar excess of  $\epsilon$ C-G (see Supplemental data, Fig. 1, and data not shown). Altogether, the data suggest that human and rat ANPG interact specifically with  $\epsilon$ C residues among all other DNA modifications tested.

Because ANPG is the only known DNA glycosylase that removes  $\epsilon$ A residues in mammalian cells, we investigated whether  $\epsilon$ C-G could inhibit ANPG in human cell-free extracts. Indeed, as shown in Fig. 1B, the addition of non-labeled  $\epsilon$ C-G to Lich cells extract completely inhibits  $\epsilon$ A excision (lanes 9 and 10), and again, it was more efficient than  $\epsilon$ A-T (lanes 3–4). A 25-fold molar excess of non-labeled A-T or 8-oxoG-C had no

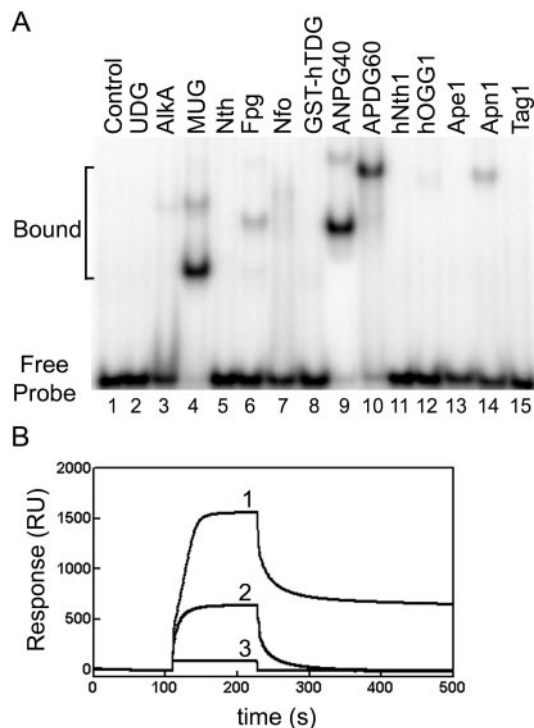


**FIG. 2. Analysis of ANPG- $\epsilon$ C interaction.** *A*, Electrophoretic mobility shift assay of various DNA repair proteins with  $\epsilon$ C-G containing duplex oligonucleotide.  $5'$ - $^{32}$ P-labeled  $\epsilon$ C-G duplex oligonucleotide (10 nM) was incubated at 0 °C for 30 min in the absence (lane 1) or presence of purified repair proteins (100 nM). *Free probe*, non-bound oligonucleotide; *bound*, enzyme-bound oligonucleotide. *B*, surface plasmon resonance analysis of the specificity of ANPG- $\epsilon$ C interaction. *Curve 1*, 60  $\mu$ l of 100 nM ANPG40 over the surface with  $\epsilon$ C-G; *curve 2*, 60  $\mu$ l of 100 nM ANPG40 was passed over the surface with C-G; *curve 3*, 60  $\mu$ l of 100 nM BSA was passed over the surface with  $\epsilon$ C-G.

effect on  $\epsilon$ A excision (lanes 6 and 8). This result suggests that  $\epsilon$ C residues, when present in DNA, inhibit  $\epsilon$ A-DNA glycosylase activity in the cell.

**Binding of Various DNA Repair Proteins to  $\epsilon$ C-G Oligonucleotide**—We proposed that the observed inhibition of ANPG-dependent DNA glycosylase activities in the presence of  $\epsilon$ C-G could result from tight and specific binding of ANPG to  $\epsilon$ C. Therefore, the interaction of  $5'$ - $^{32}$ P-labeled  $\epsilon$ C34-G with various BER proteins was examined using an EMSA. To avoid non-specific interactions, the standard binding mixture contained a 17-fold excess of BSA and a 10-fold excess of cold, non-modified 34-mer C34-G duplex oligonucleotide over labeled  $\epsilon$ C34-G. The *E. coli* MUG and human TDG proteins are  $\epsilon$ C-specific DNA glycosylases (12) and, as shown in Fig. 2A, MUG interacts in a highly specific manner with  $\epsilon$ C34-G, with more than 90% of the labeled DNA present in bound form (lane 4). In contrast, under the conditions used, GST-hTDG did not interact with  $\epsilon$ C34-G (lane 8). However, in agreement with our initial observations, the truncated human ANPG40 and rat APDG60 form a specific complex with  $\epsilon$ C34-G (lanes 9–10).

Of the other enzymes tested, UDG, Nth, hNTH1, Ape1, and Tag1 proteins did not form any complex with  $\epsilon$ C34-G (Fig. 2A, lanes 2, 5, 11, 13, and 15). However, although AlkA, Fpg, Nfo, hOGG1, and Apn1 do not excise  $\epsilon$ C, they were found to bind weakly to  $\epsilon$ C34-G (Fig. 2A, lanes 3, 6, 7, 12, and 14). Using cold competitor binding reactions, in contrast to MUG, ANPG, and APDG60, the interaction observed for AlkA, Fpg, Nfo, hOGG1, and Apn1 was found to be rather non-specific (data not shown). In conclusion, the results show that among the DNA repair proteins tested, MUG, ANPG40, and APDG60 bind to  $\epsilon$ C in a specific manner.

**TABLE I**  
ANPG proteins  $K_D$  values for  $\epsilon$ C-G and  $\epsilon$ C

Protein	$K_D^a$	
	$\epsilon$ C-G	$\epsilon$ C
	<i>nM</i>	
ANPG 40	6.1 $\pm$ 1.8	64 $\pm$ 24
ANPG 60	8.0 $\pm$ 3.6	ND <sup>b</sup>
ANPG 70	8.5 $\pm$ 3.3	ND <sup>b</sup>
ANPG 80	7.0 $\pm$ 1.4	ND <sup>b</sup>

<sup>a</sup> All values derived from EMSA and represent the mean  $\pm$  S.E. of an average of at least three separate determinations. For details, see "Experimental Procedures."

<sup>b</sup> Not determined.

**Affinity of ANPG Isoforms for  $\epsilon$ C**—To define the role of the N-terminal region of ANPG, the dissociation equilibrium constants ( $K_D$ ) of various isoforms toward  $\epsilon$ C34-G were measured using EMSA. The assay was performed under conditions where [DNA] (1 nM)  $<$   $K_D$ . As shown in Table I, the apparent  $K_D$  values of all four ANPGs are very similar, ranging from 6.1 to 8.5 nM. Surprisingly, ANPG40 also binds specifically to the  $\epsilon$ C containing single-stranded oligonucleotide. However, the affinity to single-stranded  $\epsilon$ C-DNA ( $K_D = 64$  nM) was 10 times lower than that for duplex  $\epsilon$ C-DNA (Table I).

**Surface Plasmon Resonance Analysis of the ANPG- $\epsilon$ C Interaction**—To further substantiate the specificity of the  $\epsilon$ C-ANPG interaction, an alternative to EMSA, the SPR technique, was used. Biotinylated C40-G and  $\epsilon$ C40-G oligonucleotides were immobilized onto streptavidin-coated sensor chips. ANPG40 and BSA were passed over the sensor chip surface, and the progress of binding and dissociation was measured. As shown in Fig. 2B, a strong increase in the SPR signal was observed when ANPG40 was passed over the  $\epsilon$ C40-G-sensor chip (curve 1). In contrast, no or very little binding was detected either when BSA was incubated with the  $\epsilon$ C40-G chip (curve 3) or when ANPG40 was incubated with the chip containing bound C40-G (curve 2), respectively. These results further confirm the absolute requirement of  $\epsilon$ C for specific recognition by ANPG40. To measure binding constants, the level of  $\epsilon$ C40-G on the chip was reduced to avoid possible artifacts due to mass transport limitations. Analysis of the dissociation phase profile shows that the complex formed between  $\epsilon$ C40-G and ANPG40 is extremely stable and dissociates very slowly. The calculated apparent  $K_D$  was 7.1  $\pm$  0.9 nM (the mean  $\pm$  S.E.), which is in agreement with the above EMSA data and indicates a tight and highly specific interaction between  $\epsilon$ C and ANPG.

**Inhibition of  $\epsilon$ C-DNA Glycosylase Activity by ANPG in Reconstituted System**—Next we tested the hypothesis that the protein-DNA interaction between ANPG and  $\epsilon$ C protects  $\epsilon$ C from excision by MUG and hTDG. As shown in Fig. 3, ANPG40 strongly inhibits incision of the  $\epsilon$ C-G oligonucleotide duplex by GST-hTDG (lanes 8). Interestingly, ANPG40 also weakly inhibits thymine-DNA glycosylase activity of GST-hTDG (lane 4). Inhibition of  $\epsilon$ C-DNA glycosylase activity was observed also when MUG was substituted for GST-hTDG and when ANPG70 was substituted for ANPG40 (data not shown). In conclusion, these results provide further evidence that ANPG tightly interacts with  $\epsilon$ C and forms a non-reactive enzyme-substrate complex that prevents access to the lesion by DNA repair proteins. This abortive complex is formed between the protein and the modified exocyclic base but not with the apurinic/aprimidinic site (AP site) since ANPG does not excise  $\epsilon$ C (lanes 2 and 6). It is also unlikely that ANPG specifically interacts with GST-hTDG, thus preventing the excision of  $\epsilon$ C since ANPG also inhibits the  $\epsilon$ C-DNA glycosylase activity of *E. coli* MUG.

**Development of a Direct DNA Glycosylase Assay**—In the present study, we used the fluorescence quenching mechanism

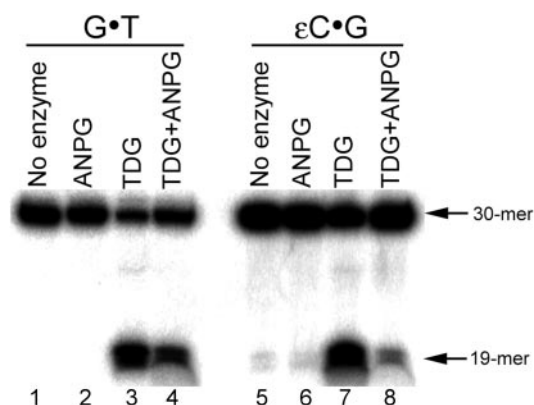


FIG. 3. Effect of ANPG40 on the excision of  $\epsilon$ C and thymine by hTDG. 10 nM 5'- $^{32}$ P-labeled  $\epsilon$ C•G (lanes 1–4) or G•T (lanes 5–8) duplexes oligonucleotides were incubated without (lanes 1 and 5) or with purified enzymes for 90 min at 30 °C. Lanes 2 and 6, 100 nM ANPG; lanes 3 and 7, 50 nM GST-hTDG; lanes 4 and 8, 100 nM ANPG and 50 nM GST-hTDG. Reaction products were analyzed as described under “Experimental Procedures.” Arrows indicate 30- and 19-mer fragments.

of molecular beacons to develop a direct BER assay. As shown in Fig. 4A, we designed a single-stranded DNA oligonucleotide, inosine-FD, containing multiple I•C nucleotides pairs labeled with a 5'-fluorescein (FITC) and a 3'-dabcyl in which the fluorophore, FITC, is held in close proximity to the quencher, dabcyl, by the stem-loop structure. In a typical molecular beacon, the quenching efficiency of the pair FITC-dabcyl is about 99.9% (43). As expected, heat denaturation of inosine-FD resulted in an enhanced fluorescence signal of up to 40-fold (data not shown). Molecular beacons undergo a spontaneous fluorogenic conformational change when they lose the stem-loop structure either during hybridization to a DNA target or during enzymatic cleavage (33, 44). Here, for the first time, we used the excision of multiple Hx residues by ANPG to disrupt base pairs in the molecular beacon and to separate the fluorophore and the quencher. As expected, incubation of inosine-FD with purified ANPG80, but not with *E. coli* Fpg or human Ape1, has led to increased fluorescence, indicating that the modified beacon can be used to specifically measure Hx-DNA glycosylase activity (Fig. 4B and data not shown). To inhibit ANPG, we designed a short, hairpin-like oligonucleotide containing either a single  $\epsilon$ C•G ( $\epsilon$ C-hairpin) or a non-modified C•G (C-hairpin) base pair. In a reconstituted system, when present at 2-fold molar excess over the protein, the C-hairpin had no effect, whereas the  $\epsilon$ C-hairpin completely inhibited the Hx-DNA glycosylase activity of ANPG80 (Fig. 4B).

**Inhibition of Hx-DNA Glycosylase Activity by  $\epsilon$ C in Cultured cells**—When introduced into living cells, molecular beacons enable real-time process monitoring (33). Here, we used molecular beacon-based DNA glycosylase assay to test whether the inhibition of ANPG by  $\epsilon$ C residues could occur in cultured mammalian cells. ANPG is the only known Hx-DNA glycosylase in mammalian cells (20, 45); therefore, inosine-FD oligonucleotides allow us to measure its activity with high specificity. The fluorescent oligonucleotide (35F-control) without a quencher residue, control non-modified oligonucleotide (35FD-control), and inosine-FD were delivered into human HeLa cells (Fig. 5) and mouse NIH3T3 fibroblasts (see Supplemental data, Fig. 2). Transfected and fixed cells were observed using fluorescence microscopy. As shown in Fig. 5, no or very low level of fluorescence was observed in control non-transfected cells (Fig. 5A) and in cells transfected with 35FD-control (Fig. 5C); in contrast, cells transfected with the 35F-control (Fig. 5B) exhibited a strong fluorescence. These observations indicate that oligonucleotides were efficiently delivered to the cells (Fig. 5B)

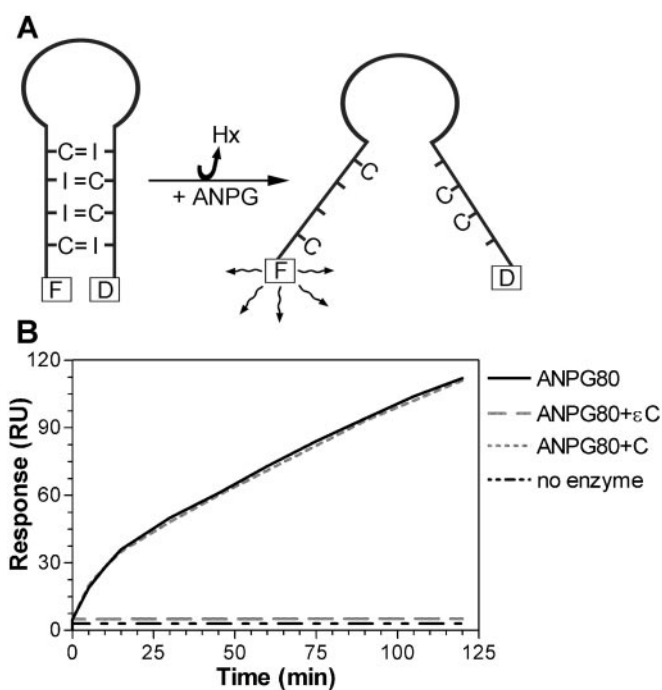


FIG. 4. A molecular beacon assay for measuring base excision repair activity. A, principle of operation of modified molecular beacon. B, activity of ANPG80 on inosine-FD, molecular beacon oligonucleotide. Fluorescence was expressed as response units (RU). 35 nM inosine-FD was incubated at 37 °C for the indicated times with or without 200 nM ANPG80 and either 400 nM C-hairpin or 400 nM  $\epsilon$ C-hairpin. For details, see “Experimental Procedures.”

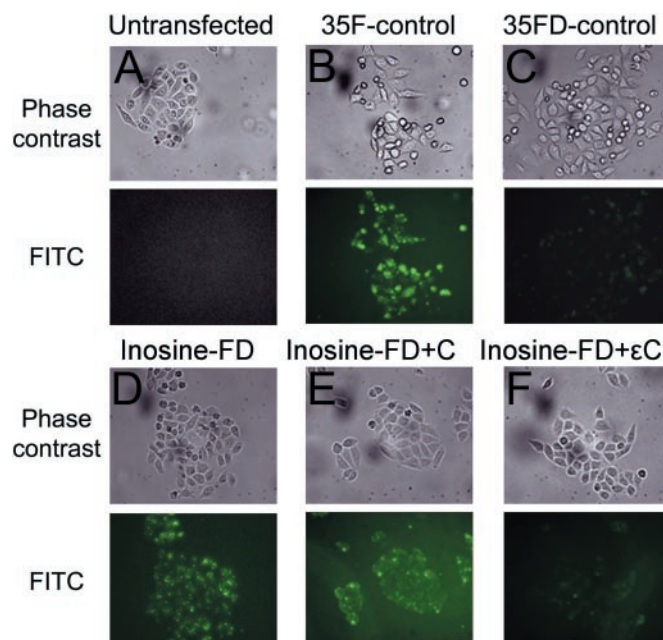
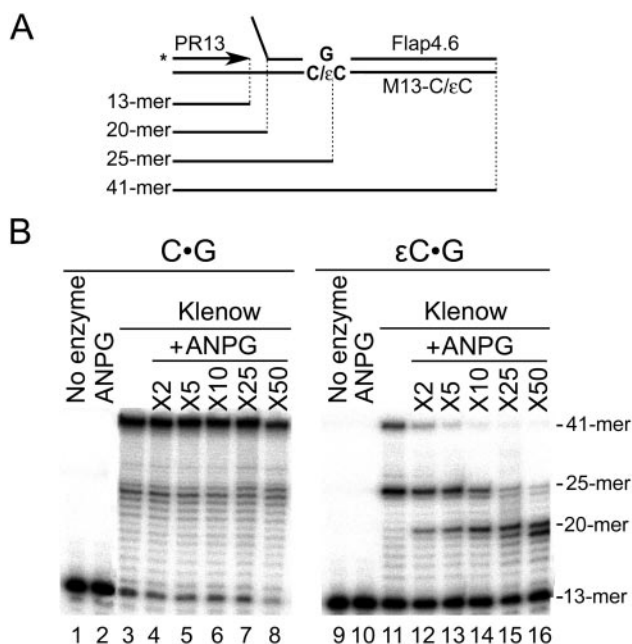


FIG. 5. Inhibition of ANPG by  $\epsilon$ C•G in cultured HeLa cells. A, non-transfected control cells; B, cells transfected with 35F-control; C, 35FD-control; D, inosine-FD; E, inosine-FD and the C-hairpin; F, inosine-FD and the  $\epsilon$ C-hairpin. HeLa cells were fixed after 5 h of transfection, and ANPG activity toward Hx residues in living cells was analyzed by fluorescence microscopy.

and that unmodified oligonucleotides are stable in cultured cells (Fig. 5C). A strong fluorescent signal was observed in the cells transfected with inosine-FD (Fig. 5D) and inosine-FD with the C-hairpin (Fig. 5E), suggesting that the molecular beacon is efficiently recognized and processed by Hx-DNA glycosylase in cultured cells. In contrast, strong enzyme inhibition, which



**FIG. 6. Effect of ANPG on DNA synthesis in primer extension assay.** A, schematic representation of the 5'-flap structure DNA template containing either a C·G or a εC·G base pair and possible elongation products: 41-mer, full-sized product; 25-mer, εC termination product; 20-mer, ANPG-εC termination product; 13-mer, 5'-<sup>32</sup>P-labeled primer. B, 10 nM 5'-<sup>32</sup>P-labeled C·G (lanes 1–8) and/or εC·G (lanes 9–16) primer/template were incubated with (lanes 3–8 and lanes 11–16) or without (lanes 1–2 and lanes 9–10) 1 unit of Klenow fragment, and the primer extension reaction was performed for 5 min at 37 °C. Lanes 1 and 9, no enzyme; lanes 2 and 10, 500 nM ANPG80; lanes 3 and 11, 10 nM ANPG80; lanes 4 and 12, 20 nM ANPG80; lanes 5 and 13, 50 nM ANPG80; lanes 6 and 14, 100 nM ANPG80; lanes 7 and 15, 200 nM ANPG80; lanes 8 and 16, 500 nM ANPG80. Reaction products were analyzed as described under “Experimental Procedures.”

kept the fluorescence near background level, was observed in cells transfected with inosine-FD and the εC-hairpin together at equimolar amounts (Fig. 5F). Similar data were obtained when using mouse NIH3T3 cells (see Supplemental data, Fig. 2). Finally, these data establish that ANPG-dependent Hx-DNA glycosylase activity is inhibited in a specific manner by εC·G both in the reconstituted systems and in the cultured cells.

**Inhibition of DNA Synthesis by the εC·ANPG Complex—**When present in DNA, εC can be bypassed by DNA polymerases (46, 47); however, we speculated that ANPG bound to εC could block DNA synthesis. As shown in Fig. 6A, a 5'-flap structure DNA template containing either C·G or εC·G base pairs was used to study the effect of ANPG80 on Klenow fragment DNA polymerase I activity. Elongation of the 5'-<sup>32</sup>P-labeled primer annealed to non-modified C·G-template by Klenow fragment generated full-sized 41-mer product (Fig. 6B, lane 3), and up to 50-fold molar excess of ANPG80 over C·G-template had no effect on polymerization (Fig. 6B, lanes 4–8). On the εC·G template, Klenow generated 41- and 25-mer fragments (Fig. 6B, lane 11) since under the conditions used, the presence of εC at position 25 created a weak termination site for the DNA polymerase. As expected, ANPG80 strongly inhibited the elongation reaction on the εC·G-template (lanes 12–16), and a significant block to the DNA polymerase was observed even at 2-fold molar excess of ANPG80 (lane 12). At 10–50-fold excess of ANPG80, the major synthesized product is a 20-mer product, suggesting that ANPG80/εC·G complex also inhibited strand displacement by Klenow. Similar results were obtained when using ANPG70 (data not shown). We also observed a strong inhibition of DNA synthesis on single-stranded εC tem-

plate at >25-fold molar excess of ANPG80 (data not shown). These results demonstrate that binding of ANPG to εC can efficiently block the DNA polymerase activity.

## DISCUSSION

The relevance of ε-adducts to chronic human disease is indicated by the finding that levels of εA and εC were significantly increased by cancer risk factors contributing to oxidative stress/LPO, such as dietary ω-6 fatty acid intake, chronic infections, and inflammatory conditions (48). The ε-adducts are removed in human cells by highly conserved DNA glycosylases (49). One of these, ANPG, excises lesions generated by certain antitumor agents and antibiotics, such as nitrosoureas and adolzelesin, thereby possibly modulating the action of these agents. The aim of the present study was to identify specific inhibitors of ANPG that might ultimately be used to modify the cell killing efficiency of different anticancer chemotherapies. By using various approaches such as competitive inhibition of enzymatic activity, EMSA, and SPR, we have shown that ANPG has a high affinity toward εC residues when present in double-stranded DNA. The enzyme has an apparent dissociation constant of  $K_D \sim 6.1$  nM for double-stranded and  $\sim 64$  nM for single-stranded εC-containing oligonucleotides. The full-length (ANPG70), spliced (ANPG60), and truncated (ANPG40 and -80) ANPG proteins have similar affinity to εC, suggesting that only the core catalytic domain of ANPG is required for εC binding. Comparison of the  $K_D$  values and the estimated molar concentration of εC in human cells (0.2–40 nM) suggests that within the nucleus, concentration of the εC·ANPG complex could easily reach the equilibrium level.

The crystal structures of ANPG80 complexed to a DNA duplex containing pyrrolidine and/or εA have been published (50, 51). ANPG80 is a single domain protein of mixed α/β structures, which forms a distinct structural group that does not resemble any other BER protein (52). Specific binding of ANPG to εC·G suggests that the enzyme recognizes εC in the active site pocket; however, in contrast to MUG and hTDG, is not able to excise the adduct. Cullinan *et al.* (53, 54) have shown by computer modeling that the εC nucleoside fits neatly into the active site of ANPG. However, these authors proposed that ANPG is not able to extrude the εC residue from duplex DNA. Based on our data, we suggest that ANPG is able to flip out εC from duplex DNA, and we speculate that it is the improper alignment of extruded adduct in the active site of ANPG that results in an inability to form a transition state intermediate structure. In support of this hypothesis, it has been demonstrated that the structure of the base pair rather than simply the damaged base plays a crucial role in base excision by ANPG (55).

The εC·ANPG abortive interaction strongly inhibits alkylpurine-, Hx-, and εA-DNA glycosylase activities of ANPG and the excision of εC by MUG and hTDG. Later observation suggests that the repair of εC in human cells might be inhibited. It is possible that the abortive εC·ANPG complex, inaccessible to BER proteins, could be processed by other DNA repair systems. For example, it has been demonstrated that the hHR23A and -B proteins, which are involved in the recognition of DNA damage in global genome-nucleotide excision repair (GG-NER) (56), interact with ANPG and elevate the rate of Hx excision (57). Therefore, the εC·ANPG complex may direct εC removal to the GG-NER pathway by recruiting the XPC-hHR23B complex to εC via an hHR23B·ANPG interaction. However, initial experiments in our laboratory have indicated only a barely detectable, if any, interaction between ANPG and hHR23A and -B under the conditions used.<sup>2</sup> Furthermore, the accumulation

<sup>2</sup> O. M. Sidorkina and J. Laval, unpublished observation.

of  $\epsilon$ A adducts induced by vinyl carbamate treatment in NER-deficient mice (XPC<sup>-/-</sup>, and XPA<sup>-/-</sup>) does not significantly differ from that of wild type, suggesting that NER pathway is not involved in the repair of  $\epsilon$ -bases.<sup>3</sup>

The  $\epsilon$ C-ANPG complex strongly inhibits BER in reconstituted systems, suggesting that in living cells, the repair of alkylated purines, Hx and  $\epsilon$ A, would also be perturbed. To substantiate the role of this interaction in living cells, we have developed for the first time a direct DNA repair assay based on molecular beacon oligonucleotides containing modified residues, which does not require incision of the phosphodiester backbone and which allows direct and high throughput measurements to be obtained both in reconstituted systems and in living cells. Inosine-FD, a stem-loop oligonucleotide containing multiple Hx residues and labeled with fluorophore and quencher, was used as the substrate for cellular ANPG. The inosine-FD probe was introduced into HeLa and NIH3T3 cells, and the resulting DNA glycosylase-mediated excision of Hx led to an enhancement of fluorescence. However, when inosine-FD and the  $\epsilon$ C-hairpin oligonucleotide were transfected together, no fluorescence was observed. As expected, transfection of the control, the C-hairpin oligonucleotide, had no effect on fluorescence. This result demonstrates that  $\epsilon$ C-ANPG complex may occur in mammalian cells under certain conditions.

Finally, the effect of the  $\epsilon$ C-ANPG interaction on a DNA polymerase was studied using primer extension assays. We demonstrated that binding of ANPG to double- or single-stranded DNA containing an  $\epsilon$ C residue strongly inhibits DNA synthesis by the *E. coli* Klenow fragment of DNA polymerase I. This result suggests that *in vivo*,  $\epsilon$ C residues could be more genotoxic than  $\epsilon$ A. Therefore, hijacking of ANPG by  $\epsilon$ C residues could be an important determinant of  $\epsilon$ -adduct genotoxicity, and the following observations lend support for this hypothesis: (i) somatic instability of the CAG repeat in Huntington disease is based on *hijacking* of the mismatch repair protein Msh2 by DNA loop endogenously formed in the repeat region (58, 59); (ii) the cell killing potency of DNA adducts generated by cisplatin is mediated by hijacking of the high mobility group domain proteins (60); (iii) the levels of  $\epsilon$ A induced exogenously by vinyl chloride and vinyl carbamate are much higher than those of  $\epsilon$ C (61); in contrast, the ratio of  $\epsilon$ -adducts generated by endogenous LPO could be shifted toward  $\epsilon$ C formation. It has been demonstrated that in ulcerative colitis, a chronic inflammatory condition associated with a predisposition to colon cancer,  $\epsilon$ C levels were higher than in normal colon, whereas  $\epsilon$ A was lower (62); also, in colon cancer biopsies, the level of  $\epsilon$ C was 30 times higher than that of  $\epsilon$ A (63). Recently, it has been shown that inflammation in ulcerative colitis is correlated with an increased level of ANPG, which in turn produces instability at microsatellite sequences in various types of cells in the affected tissue (64). Based on these observations, we propose that abortive repair of LPO-induced  $\epsilon$ C may have profound biological implications.

In summary, the results obtained in the present study demonstrate that ANPG has a dual role in the repair of  $\epsilon$ -adducts. It excises  $\epsilon$ A and 1,N<sup>2</sup>- $\epsilon$ G, but at the same time, it can prevent the repair of  $\epsilon$ C by forming an abortive protein-DNA complex. The data suggest a novel mode of recognition of damaged bases by a DNA glycosylase and an unexpected mechanism by which the repair of  $\epsilon$ -adducts can be modulated in mammalian cells. Thus, the genotoxicity of  $\epsilon$ C *in vivo* can be enhanced by hijacking of the DNA glycosylase, suggesting that increased endogenous LPO could be extremely harmful to human cells. It is tempting to speculate that oxidation of lipids in the blood-

stream and in the colon tissues may lead to increased levels of  $\epsilon$ C, which in turn hijacks ANPG, and that this abortive repair complex could trigger chronic inflammation observed in atherosclerosis and in ulcerative colitis (64, 65). In conclusion, the present data may provide insight to molecular genotoxicity of LPO, which is likely to be a causative factor in a number of human degenerative disorders.

**Acknowledgments**—We thank Dr. Yakov Alekseev (Syntol, Moscow, Russia) for inosine-FD oligonucleotide synthesis, Drs. Helmut Bartsch, Jagadeesan Nair, and Alain Barbin for helpful discussions and providing data prior to publication, and Drs. Rhoderick Elder and Jean-Marie Saucier for critical reading of the manuscript.

## REFERENCES

- Nair, J., Barbin, A., Guichard, Y., and Bartsch, H. (1995) *Carcinogenesis* **16**, 613–617
- Chung, F. L., Chen, H. J., and Nath, R. G. (1996) *Carcinogenesis* **17**, 2105–2111
- Pollack, M., Oe, T., Lee, S. H., Silva Elipse, M. V., Arison, B. H., and Blair, I. A. (2003) *Chem. Res. Toxicol.* **16**, 893–900
- Barbin, A. (2000) *Mutat. Res.* **462**, 55–69
- Marnett, L. J., and Burcham, P. C. (1993) *Chem. Res. Toxicol.* **6**, 771–785
- Nair, J. (1999) *IARC Sci. Publ.* **150**, 55–61
- Mertens, A., Verhamme, P., Bielicki, J. K., Phillips, M. C., Quarck, R., Verreth, W., Stengel, D., Ninio, E., Navab, M., Mackness, B., Mackness, M., and Holvoet, P. (2003) *Circulation* **107**, 1640–1646
- Basu, A. K., Wood, M. L., Niedernhofer, L. J., Ramos, L. A., and Essigmann, J. M. (1993) *Biochemistry* **32**, 12793–12801
- Moriya, M., Zhang, W., Johnson, F., and Grollman, A. P. (1994) *Proc. Natl. Acad. Sci. U. S. A.* **91**, 11899–11903
- Pandya, G. A., and Moriya, M. (1996) *Biochemistry* **35**, 11487–11492
- Levine, R. L., Yang, I. Y., Hossain, M., Pandya, G. A., Grollman, A. P., and Moriya, M. (2000) *Cancer Res.* **60**, 4098–4104
- Saparbaev, M., and Laval, J. (1998) *Proc. Natl. Acad. Sci. U. S. A.* **95**, 8508–8513
- Hang, B., Medina, M., Fraenkel-Conrat, H., and Singer, B. (1998) *Proc. Natl. Acad. Sci. U. S. A.* **95**, 13561–13566
- Petronzelli, F., Riccio, A., Markham, G. D., Seeholzer, S. H., Genuardi, M., Karbowski, M., Yeung, A. T., Matsumoto, Y., and Bellacosa, A. (2000) *J. Cell. Physiol.* **185**, 473–480
- Kavli, B., Sundheim, O., Akbari, M., Otterlei, M., Nilsen, H., Skorpen, F., Aas, P. A., Hagen, L., Krokan, H. E., and Slupphaug, G. (2002) *J. Biol. Chem.* **277**, 39926–39936
- Gros, L., Saparbaev, M. K., and Laval, J. (2002) *Oncogene* **21**, 8905–8925
- O'Connor, T. R., and Laval, J. (1990) *EMBO J.* **9**, 3337–3342
- Engelward, B. P., Boosalis, M. S., Chen, B. J., Deng, Z., Siciliano, M. J., and Samson, L. D. (1993) *Carcinogenesis* **14**, 175–181
- Engelward, B. P., Dreslin, A., Christensen, J., Huszar, D., Kurahara, C., and Samson, L. (1996) *EMBO J.* **15**, 945–952
- Engelward, B. P., Weeda, G., Wyatt, M. D., Broekhof, J. L., de Wit, J., Donker, I., Allan, J. M., Gold, B., Hoeijmakers, J. H., and Samson, L. D. (1997) *Proc. Natl. Acad. Sci. U. S. A.* **94**, 13087–13092
- Elder, R. H., Jansen, J. G., Weeks, R. J., Willington, M. A., Deans, B., Watson, A. J., Mynett, K. J., Bailey, J. A., Cooper, D. P., Rafferty, J. A., Heeran, M. C., Wijnhoven, S. W., van Zeeland, A. A., and Margison, G. P. (1998) *Mol. Cell. Biol.* **18**, 5828–5837
- Roth, R. B., and Samson, L. D. (2002) *Cancer Res.* **62**, 656–660
- Cardinal, J. W., Margison, G. P., Mynett, K. J., Yates, A. P., Cameron, D. P., and Elder, R. H. (2001) *Mol. Cell. Biol.* **21**, 5605–5613
- Cerda, S. R., Turk, P. W., Thor, A. D., and Weitzman, S. A. (1998) *FEBS Lett.* **431**, 12–18
- Vickers, M. A., Vyas, P., Harris, P. C., Simmons, D. L., and Higgs, D. R. (1993) *Proc. Natl. Acad. Sci. U. S. A.* **90**, 3437–3441
- Pendlebury, A., Frayling, I. M., Santibanez Koref, M. F., Margison, G. P., and Rafferty, J. A. (1994) *Carcinogenesis* **15**, 2957–2960
- O'Connor, T. R., and Laval, J. (1991) *Biochem. Biophys. Res. Commun.* **176**, 1170–1177
- O'Connor, T. R. (1993) *Nucleic Acids Res.* **21**, 5561–5569
- Saparbaev, M., Langouet, S., Privezentzev, C. V., Guengerich, F. P., Cai, H., Elder, R. H., and Laval, J. (2002) *J. Biol. Chem.* **277**, 26987–26993
- Scharer, O. D., Nash, H. M., Jiricny, J., Laval, J., and Verdine, G. L. (1998) *J. Biol. Chem.* **273**, 8592–8597
- Bessho, T., Roy, R., Yamamoto, K., Kasai, H., Nishimura, S., Tano, K., and Mitra, S. (1993) *Proc. Natl. Acad. Sci. U. S. A.* **90**, 8901–8904
- Kartalou, M., Samson, L. D., and Essigmann, J. M. (2000) *Biochemistry* **39**, 8032–8038
- Tyagi, S., and Kramer, F. R. (1996) *Nat. Biotechnol.* **14**, 303–308
- Stryer, L. (1978) *Annu. Rev. Biochem.* **47**, 819–846
- Kartalou, M., and Essigmann, J. M. (2001) *Mutat. Res.* **478**, 1–21
- Kovtun, I. V., Goellner, G., and McMurray, C. T. (2001) *Biochem. Cell Biol.* **79**, 325–336
- Saparbaev, M., and Laval, J. (1994) *Proc. Natl. Acad. Sci. U. S. A.* **91**, 5873–5877
- Lefebvre, P., Zak, P., and Laval, J. (1993) *DNA Cell Biol.* **12**, 233–241
- Ishchenko, A. A., Sanz, G., Privezentzev, C. V., Maksimenko, A. V., and Saparbaev, M. (2003) *Nucleic Acids Res.* **31**, 6344–6353
- Ye, N., Holmquist, G. P., and O'Connor, T. R. (1998) *J. Mol. Biol.* **284**, 269–285
- Saparbaev, M., Kleibl, K., and Laval, J. (1995) *Nucleic Acids Res.* **23**,

<sup>3</sup> A. Barbin, personal communication.

- 3750–3755
42. Asaeda, A., Ide, H., Asagoshi, K., Matsuyama, S., Tano, K., Murakami, A., Takamori, Y., and Kubo, K. (2000) *Biochemistry* **39**, 1959–1965
43. Tyagi, S., Bratu, D. P., and Kramer, F. R. (1998) *Nat. Biotechnol.* **16**, 49–53
44. Rizzo, J., Gifford, L. K., Zhang, X., Gewirtz, A. M., and Lu, P. (2002) *Mol. Cell. Probes* **16**, 277–283
45. Hang, B., Singer, B., Margison, G. P., and Elder, R. H. (1997) *Proc. Natl. Acad. Sci. U. S. A.* **94**, 12869–12874
46. Simha, D., Yadav, D., Rzepka, R. W., Palejwala, V. A., and Humayun, M. Z. (1994) *Mutat. Res.* **304**, 265–269
47. Guliaev, A. B., Hang, B., and Singer, B. (2002) *Nucleic Acids Res.* **30**, 3778–3787
48. Bartsch, H., and Nair, J. (2000) *Toxicology* **153**, 105–114
49. Gros, L., Ishchenko, A. A., and Saparbaev, M. (2003) *Mutat. Res.* **531**, 219–229
50. Lau, A. Y., Scharer, O. D., Samson, L., Verdine, G. L., and Ellenberger, T. (1998) *Cell* **95**, 249–258
51. Lau, A. Y., Wyatt, M. D., Glassner, B. J., Samson, L. D., and Ellenberger, T. (2000) *Proc. Natl. Acad. Sci. U. S. A.* **97**, 13573–13578
52. Hollis, T., Lau, A., and Ellenberger, T. (2000) *Mutat. Res.* **460**, 201–210
53. Cullinan, D., Johnson, F., Grollman, A. P., Eisenberg, M., and de los Santos, C. (1997) *Biochemistry* **36**, 11933–11943
54. Cullinan, D., Johnson, F., and de los Santos, C. (2000) *J. Mol. Biol.* **296**, 851–861
55. Abner, C. W., Lau, A. Y., Ellenberger, T., and Bloom, L. B. (2001) *J. Biol. Chem.* **276**, 13379–13387
56. Sugawara, K., Ng, J. M., Masutani, C., Maekawa, T., Uchida, A., van der Spek, P. J., Eker, A. P., Rademakers, S., Visser, C., Aboussekhra, A., Wood, R. D., Hanaoka, F., Bootsma, D., and Hoeijmakers, J. H. (1997) *Mol. Cell. Biol.* **17**, 6924–6931
57. Miao, F., Bouziane, M., Dammann, R., Masutani, C., Hanaoka, F., Pfeifer, G., and O'Connor, T. R. (2000) *J. Biol. Chem.* **275**, 28433–28438
58. Manley, K., Shirley, T. L., Flaherty, L., and Messer, A. (1999) *Nat. Genet.* **23**, 471–473
59. Kovtun, I. V., and McMurray, C. T. (2001) *Nat. Genet.* **27**, 407–411
60. Kartalou, M., and Essigmann, J. M. (2001) *Mutat. Res.* **478**, 23–43
61. Marion, M. J., and Boivin-Angele, S. (1999) *IARC Sci. Publ.* 315–324
62. Bartsch, H., and Nair, J. (2002) *Cancer Detect. Prev.* **26**, 308–312
63. Bartsch, H., Nair, J., and Owen, R. W. (2002) *Biol. Chem.* **383**, 915–921
64. Hofseth, L. J., Khan, M. A., Ambrose, M., Nikolayeva, O., Xu-Welliver, M., Kartalou, M., Hussain, S. P., Roth, R. B., Zhou, X., Mechanic, L. E., Zurer, I., Rotter, V., Samson, L. D., and Harris, C. C. (2003) *J. Clin. Invest.* **112**, 1887–1894
65. Feng, B., Yao, P. M., Li, Y., Devlin, C. M., Zhang, D., Harding, H. P., Sweeney, M., Rong, J. X., Kuriakose, G., Fisher, E. A., Marks, A. R., Ron, D., and Tabas, I. (2003) *Nat. Cell Biol.* **5**, 781–792